

Observation of Spin-Charge Separation in One-Dimensional SrCuO₂

C. Kim,¹ A. Y. Matsuura,¹ Z.-X. Shen,¹ N. Motoyama,² H. Eisaki,² S. Uchida,² T. Tohyama,³ and S. Maekawa^{4,5}
¹*Department of Applied Physics and Stanford Synchrotron Radiation Laboratory, Stanford University, Stanford, California 94305*
²*Department of Superconductivity, The University of Tokyo, Yayoi 2-11-16, Bunkyo-ku, Tokyo 133, Japan*
³*Department of Physics, Faculty of Education, Mie University, Tsu 514, Japan*
⁴*Department of Applied Physics, Nagoya University, Nagoya 464-01, Japan*
⁵*Institute for Materials Research, Tohoku University, Sendai 980-77, Japan*

(Received 29 April 1996)

Angle-resolved photoemission data from one-dimensional SrCuO₂ compounds are found to be qualitatively different from that of two-dimensional Sr₂CuO₂Cl₂. The data can be quantitatively accounted for by the exact diagonalization calculation based on the t - J model. We identify the two underlying bands having approximately 1.2 and 0.3 eV energy dispersion as that of holon and spinon, with their energy scaled by t and J , respectively. [S0031-9007(96)01554-2]

PACS numbers: 71.27.+a, 78.20.Bh, 79.60.Bm,

Stimulated by the discovery of high- T_c superconductors, there is renewed interest in the properties of low dimensional systems. A particular system that has attracted much recent attention is the one-dimensional (1D) copper-oxide chain and ladder compounds [1–3]. It is believed that the quasiparticles in the Fermi liquid sense do not exist in the 1D case. Lieb and Wu found that the low energy physics is dominated by uncoupled collective modes of spin and charge excitations [4], now often called spinons and holons. The decoupled nature of these collective modes implies that the spin and charge degrees of freedom of real electrons, as represented by the spinon and holon, are separated—an important idea that has also been used to try to explain the properties of 2D cuprate superconductors [5]. In this sense, the spinon and holon are new elementary particles (excitations) in the 1D solid. Their conceptual importance is the same as that of other elementary particles in solids such as phonons and magnons. Various experimental attempts have been made to observe these new particles [6–8]. So far, no direct, unambiguous evidence of spin-charge separation in quantitative agreement with theoretical calculations has been found.

In this Letter, we report angle-resolved photoemission (ARPES) data from the 1D copper-oxide chain compound SrCuO₂. The ARPES data show distinct one-dimensional behavior. Along the chain direction, we see significant dispersion with the features reaching the highest energy at $\pi/2$ and the lowest energy near the Γ and π points. A comparison of our 1D data with those of the 2D Sr₂CuO₂Cl₂ compound [9] reveals a striking contrast. The total dispersion in the 1D case is more than 1 eV compared to only ~ 0.3 eV in the 2D case. No dramatic intensity drop is observed in the 1D case when going from less than $\pi/2$ to above $\pi/2$, while more than a factor of 10 is observed in the 2D case. These aspects of the data can be quantitatively accounted for by numerical simulations using the t - J model with the t and J parameters constrained by other experiments and calculations. The key reason for the difference between the 1D and 2D results is that

the spin-charge separation is realized in the 1D case. In particular, we identify the most prominent feature, with more than 1 eV dispersion from $\pi/2$ to π , as the holon band scaled by t . This band does not exist in the 2D case because the hole motion is coupled with the spin background. We identify the lower bound of the dispersive features, with 0.3 eV dispersion, as the spinon band scaled by J .

SrCuO₂ is a charge transfer insulator with a 1.8 eV gap as determined by optical measurements [10]. The chains are formed by continuous 180° Cu-O-Cu bonds, and they are coupled through 90° Cu-O-Cu bonds [11]. The 1D nature of this compound is confirmed by NMR [12] and magnetization measurements [11]. The single crystals of SrCuO₂ were synthesized by the traveling-solvent-floating-zone (TSFZ) method using CuO as the flux. The details of the crystal growth are described elsewhere [11]. The obtained single crystals have clear facets along the a - c plane and are easily cleaved along this plane. The magnetic susceptibility data on these single crystals are in excellent agreement with theoretical calculation [13] in the temperature range from 20 to 800 K. This calculation produces an antiferromagnetic (AF) exchange coupling of $J = 2100 \pm 200$ K, which shows that the system can be regarded as an ideal 1D AF system in this temperature-energy scale [11].

Experiments were performed at the undulator beam line V at the Stanford Synchrotron Radiation Laboratory (SSRL). The samples were cleaved *in situ*, and the base pressure of the chamber was better than 5×10^{-11} Torr. The overall system energy resolution, including both the beam line and the analyzer, was 75 meV. The angular resolution of the system is $\pm 1^\circ$, or better than $\pm(1/20)\pi$ in k with $h\nu = 22.4$ eV. Data presented here are from freshly cleaved samples at room temperature.

ARPES shows the filled states of SrCuO₂ below the charge transfer gap. It has a wide main valence band peak with a small foot on the higher kinetic energy side. The main valence band has a few peaks and its overall shape

is similar to other cuprates. Only the foot region of the data is presented here since we are interested in low energy physical properties. Figure 1 shows two sets of spectra at different k positions along the chain direction, with the number on each spectrum representing the k position in units of π/a ($1 = \pi/a$). The left panel has spectra from k positions between the Γ and $\pi/2$ points, and the right panel has spectra from positions between $\pi/2$ and π . Spectra in the right panel show that there is a main feature with a maximum at $\pi/2$. It merges into the main valence band with an estimated dispersion of more than 1 eV. A very weak feature is observed at 0.1 eV near the π point. By contrast, the spectra in the left panel have a broad, non-Lorentzian feature whose centroid disperses about 0.5 eV. The broadness and the subtle line shape modulation of the feature between Γ and $\pi/2$ lead us to believe that the data consist of more than one component. From $\pi/2$ to Γ , the centroid of the feature appears to give a band which disperses to the lower kinetic energy side and folds back around 0.23π . Since there is no symmetry reason for this band folding, it can be better understood as existence of multiple features. Estimation of the peak position on this side is greatly hampered by the strong feature from the main valence band. As we can see in the figure, any peak that exists beyond 0.8 eV would be hardly noticeable at the Γ point as the top of the main valence band moves toward

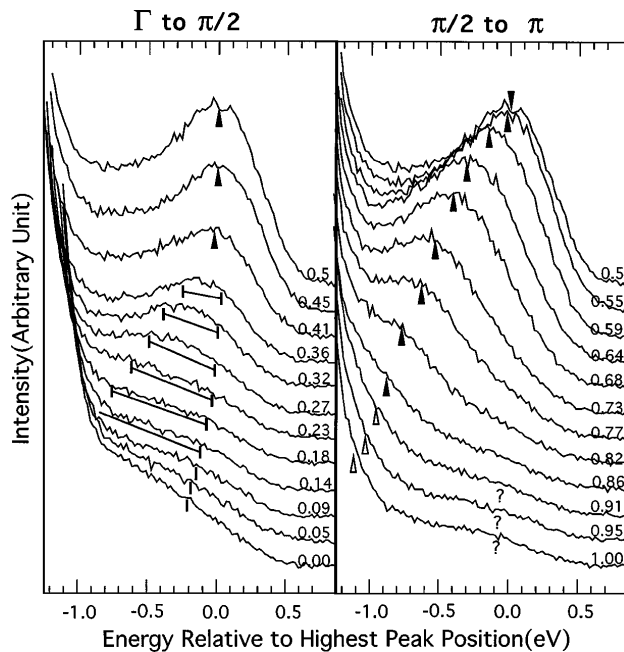


FIG. 1. ARPES spectra from SrCuO_2 . The left panel has spectra from k positions between Γ and $\pi/2$ and the right panel from $\pi/2$ to π . Different marks are guides to the eye. The solid triangles are used for the peaks which are certain and the question marks when there is some ambiguity (refer to the main text). The spectra in the left panel show a broad feature which implies that there may exist multiple features. The line segments indicate the upper and lower bounds for the dispersive features.

higher kinetic energy. We have also taken spectra along the direction perpendicular to the chain (not reported here) which show much smaller dispersion (total dispersion less than 0.15 eV) confirming the predominant 1D nature of the copper oxide chain in the electronic structure.

In Fig. 2, the E vs k relationship is plotted in the left panel. For the two distinct features from $\pi/2$ to π , the less dispersive feature near the π point is marked with question marks, for a reason discussed later. Meanwhile, the error bars between Γ and $\pi/2$ represent a rough estimate of the area where features may exist, with the thick lines indicating the upper and lower bounds of dispersive features. Again, the error bar is particularly large near Γ because the features are further complicated by the emissions from the main valence band. For comparison, experimental data from 2D $\text{Sr}_2\text{CuCl}_2\text{O}_2$ is plotted in the right panel. The data cannot be explained by a simple band calculation.

In order to understand the data, we examine the t - J model which is one of the canonical models to describe the low energy properties in the cuprates. The Hamiltonian is given by

$$H_{ij} = -t \sum_{\langle i,j \rangle \sigma} (\tilde{c}_{i\sigma}^\dagger \tilde{c}_{j\sigma} + \text{H.c.}) + J \sum_{\langle i,j \rangle} (\mathbf{S}_i \cdot \mathbf{S}_j - \frac{1}{4} n_{i\uparrow} n_{j\downarrow}), \quad (1)$$

where $\tilde{c}_{i\sigma} = c_{i\sigma}(1 - n_{i\bar{\sigma}})$ is the annihilation operator of an electron with spin σ at site i , $n_{i\sigma} = c_{i\sigma}^\dagger c_{i\sigma}$, \mathbf{S}_i is the spin operator at site i with $S = \frac{1}{2}$, and $n_i = n_{i\uparrow} + n_{i\downarrow}$. The summation $\langle i, j \rangle$ runs over nearest neighbor pairs.

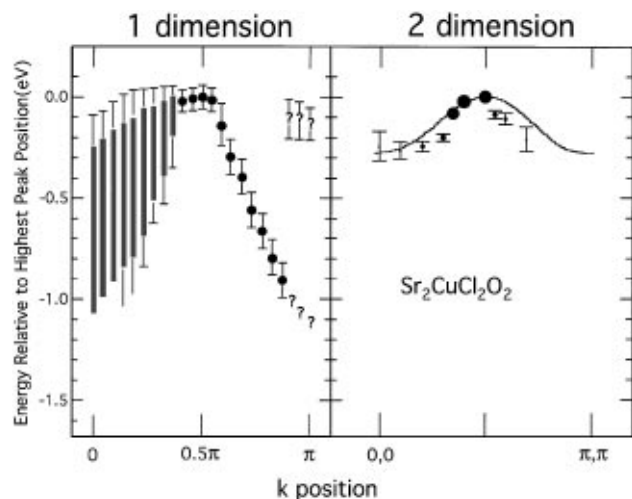


FIG. 2. E vs k relationship for the 1D and 2D (from Ref. [8]). For the 1D case, there are two bands between $\pi/2$ and π with the less dispersive band marked with question marks for the same reason as in Fig. 1. Between Γ and $\pi/2$, the thick lines are the upper and lower bounds of the dispersive features. For the 2D case, there is only one band with the sizes of the circles approximately representing the spectral weights.

In the uniform susceptibility measurements of SrCuO₂, a 0.18 eV antiferromagnetic exchange interaction J has been obtained [11], whereas the value $J = 0.23$ eV was given by the optical absorption measurements [10]. A rounded value of 0.2 eV was used in the calculation. The hopping parameter t was determined to be $t = 0.60$ eV by taking the ratio $t/J = 3$, the ratio for other cuprates [14]. The spectrum for electron removal is expressed as

$$A(k, \omega) = \sum_{\nu\sigma} |\langle \nu | c_{k\sigma} | 0 \rangle|^2 \delta(\omega + E_\nu - E_0), \quad (2)$$

where ν denotes the ν th eigenvector with eigenvalue E_ν and $|0\rangle$ denotes the ground state with energy E_0 , and $c_{k\sigma} = L^{-1/2} \sum_i c_{i\sigma} e^{ikR_i}$. L is the total number of sites. We have calculated the spectrum by the numerical exact diagonalization technique in a 1D cluster with $L = 22$ and with periodic boundary conditions.

Figure 3(a) shows the spectrum obtained by the standard Lanczos procedure with Lorentzian broadening of $0.01t$. The highest energy excitation appears at $k = 5\pi/11$. We find that the spectrum is in strong contrast with those of 2D insulator studies [15–17], and has the following features: (i) between $k = 4\pi/11$ and π a sharp edge is seen, (ii) between $k = 0$ and $3\pi/11$ the spectra

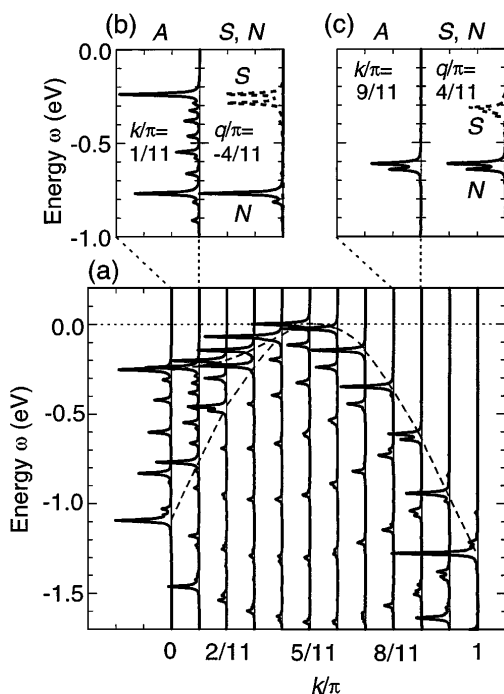


FIG. 3. (a) Spectral function $A(k, \omega)$ for a t - J ring of 22 sites with $J = 0.2$ eV and $t = 0.6$ eV. The momentum k is defined as $n\pi/11$, n being an integer. The energy ω is measured from the highest energy peak at $k = 5\pi/11$. The δ functions are convolved with a Lorentzian broadening of $0.01t$. The broken lines guide the eye. (b) $A(k, \omega)$ with $k = \pi/11$, and the dynamic spin and charge correlation functions, $S(q, \omega)$ (dashed line) and $N(q, \omega)$ (solid line), with $q = k - 5\pi/11$. The energy ω of S and N is converted into $-\omega$. (c) The same as (b), with $k = 9\pi/11$.

have a two edge structure, and (iii) there exist dense spectra between these edges. These features are consistent with the observed spectrum in SrCuO₂. The agreement of their energy scale is also striking.

In order to study the nature of the spectrum, we calculate the dynamic spin and charge correlation functions, $S(q, \omega)$ and $N(q, \omega)$, in the 21 electron system to which the final state for the electron removal spectrum belongs [18]. In Fig. 3(b), $A(k, \omega)$ with $k = \pi/11$ is compared with $S(q, \omega)$ and $N(q, \omega)$ where $q = k - 5\pi/11$ is the momentum transfer. We find that the high energy edge of $A(k, \omega)$ is related to the spin excitation, while the low energy edge is due to the charge excitation. In Fig. 3(c), $A(k, \omega)$ with $k = 9\pi/11$ is replotted together with $S(q, \omega)$ and $N(q, \omega)$. The significant weight of $A(k, \omega)$ is given by the charge excitation, in contrast with that for $k \leq 3\pi/11$. We note that although there exists a spin excitation around -0.3 eV, the intensity of $A(k, \omega)$ is very weak.

By examining the Lieb-Wu equations [4] for the Bethe-ansatz solution of the 1D Hubbard model with strong interactions, we may obtain the excitation energies. The equations show that there is a spinon excitation between 0 and $k = \pi/2$ which is proportional to the wave number around $k = \pi/2$ and has the energy $\pi J/2$ at $k = 0$. On the other hand, the holon excitation is proportional to the square of the wave number around $k = \pi/2$ and has the relation $\omega = 2t(\sin k - 1)$. There also exists an area between $k = \pi/2$ and 0 where the mixed excitations of spinons and holons are densely distributed. These features are consistent with the numerical results shown in Fig. 3. In the strong interaction limit in the 1D Hubbard model ($J \rightarrow 0$ in the t - J model), the shape of the spectrum has been obtained [19], which may also be compared with Fig. 3(a).

From the above discussion, most of the spectra observed in SrCuO₂ can be understood quantitatively as the spinon and holon excitations in the 1D t - J model. The broad excitation from Γ to $\pi/2$ is a mixture of spinon and holon excitations with lower and upper bounds being set by spinon and holon excitations, respectively. The very dispersive band from $\pi/2$ to π , which is the most prominent feature in the data, is the holon excitation band. We have also performed calculations with some coupling between the chains. These calculations show that the above results hold even when the chain coupling is accounted for, indicating that the small dispersion observed perpendicular to the chain will not affect our conclusions. However, the theory does not reproduce the small spectral weight around $k = \pi$ in the high energy region (question marks), although spinon excitations exist in the region. We believe that the small spectral weight at the π point is not real but a “leftover” due to elastic and inelastic scattering. As often seen in ARPES data, one usually sees a peaklike feature at E_F even when the real peak disperses past E_F . Another possibility is the thermal effect. At finite temperatures, the edge structure is smeared out, and

spectral weight might be transferred to the high energy region. These effects could contribute to the enhancement of the spectral weight around $k = \pi$.

The spin-charge separation in the 1D system is also the natural explanation for the striking difference between the present data and those from the 2D $\text{Sr}_2\text{CuO}_2\text{Cl}_2$ [9]: (i) As plotted in Fig. 2, the 2D case has only the narrow band which is scaled by J , while we do not see a distinct band scaled by t , as observed in 1D. (ii) The band in the 2D case shows a dramatic drop in intensity when moving from below $(\pi/2, \pi/2)$ to above $(\pi/2, \pi/2)$, a behavior not present in the 1D case. (iii) The features in the 2D case can be reasonably explained by a broadened Lorentzian while this cannot be done for the 1D features. These effects can naturally be explained by the fact that the single hole motion in the 2D insulator is coupled to the spin background, resulting in the holon band being completely incoherent. Thus, the qualitatively different behavior seen in the 1D and 2D cases is a strong indication that the spin-charge separation is indeed realized in our experiments on SrCuO_2 . The clear manifestation of this effect that distinguishes this work from other studies on metallic samples [6–8] may be attributed to two effects: (i) the unusually large J value and (ii) the present experiment investigates a single hole in an insulator.

We acknowledge stimulating discussions with B. O. Wells, R. L. Laughlin, P. W. Anderson, E. Dagotto, S. Haas, H. Shiba, and M. Takigawa. Photoemission experiments were performed at SSRL which is operated by the DOE office of Basic Energy Research, Division of Chemical Sciences. The office's division of Material Science provided support for this research. This work has been supported by the New Energy and Industrial Technology Development Organization (NEDO) and Priority-Areas Grants from the Ministry of Education, Science and Culture of Japan. The Stanford work was also supported by NSF Grant No. 9311566 and the NSF grant through the Center for Materials Research. The Tokyo work was also supported by the NEDO grant for Advanced Industrial Technology Research. The Computation was done using the facilities of the supercomputer

center, Institute of Solid State Physics, University of Tokyo.

-
- [1] A. Keren *et al.*, Phys. Rev. B **48**, 12 926 (1993).
 - [2] M. Takano, Z. Hiroi, M. Azuma, and Y. Takeda, J. Appl. Phys. Ser. **7**, 3 (1992).
 - [3] E. Dagotto and T. M. Rice, Science **271**, 618 (1996).
 - [4] E. H. Lieb and F. Y. Wu, Phys. Rev. Lett. **20**, 1445 (1968).
 - [5] P. W. Anderson, *A Career in Theoretical Physics*, World Scientific Series in 20th Century Physics (World Scientific, Singapore, 1994), Vol. 7.
 - [6] B. Dardel, D. Malterre, M. Grioni, P. Weibel, Y. Baer, and F. Levy, Phys. Rev. Lett. **67**, 3144 (1991).
 - [7] A. Sekiya *et al.*, Phys. Rev. B **51**, 13 899 (1995); M. Nakamura *et al.*, Phys. Rev. B **49**, 16 191 (1994).
 - [8] J. W. Allen, G.-H. Gweon, R. Claessen, and K. Matho, J. Phys. Chem. Solids **56**, 1849 (1995); R. Claessen *et al.*, J. Electron Spectrosc. Relat. Phenom. **76**, 121 (1995).
 - [9] B. O. Wells *et al.*, Phys. Rev. Lett. **74**, 964 (1995).
 - [10] H. Yasuhara and Y. Tokura (private communication).
 - [11] N. Motoyama, H. Eisaki, and S. Uchida, Phys. Rev. Lett. **76**, 3212 (1996).
 - [12] M. Takigawa *et al.* (unpublished).
 - [13] S. Eggert, I. Affleck, and M. Takahashi, Phys. Rev. Lett. **73**, 332 (1994).
 - [14] Our resonant photoemission study on this compound shows that the basic electronic structure is similar to that of other cuprate superconductors. For resonant photoemission studies on other cuprates, refer to O. Gunnarsson *et al.*, Phys. Rev. B **41**, 4811 (1990).
 - [15] A. Nazarenko, K. J. E. Vos, S. Haas, E. Dagotto, and R. J. Gooding, Phys. Rev. B **51**, 8676 (1995).
 - [16] S. Haas, A. Moreo, and E. Dagotto, Phys. Rev. Lett. **74**, 4281 (1995).
 - [17] P. W. Leung and R. J. Gooding, Phys. Rev. B **52**, R15 711 (1995).
 - [18] T. Tohyama and S. Maekawa, J. Phys. Soc. Jpn. **65**, 1902 (1996).
 - [19] M. Ogata and H. Shiba, Phys. Rev. B **41**, 2326 (1990); S. Sorella and A. Parola, J. Phys. Condens. Matter. **4**, 3589 (1992).